Hindawi Publishing Corporation
Journal of Nanomaterials
Volume 2014, Article ID 409493, 7 pages
http://dx.doi.org/10.1155/2014/409493

Research Article

Electroluminescent Devices Based on Junctions of Indium Doped Zinc Oxide and Porous Silicon

F. Severiano,[1] G. García,[2] L. Castañeda,[3] J. M. Gracia-Jiménez,[1] Heberto Gómez-Pozos,[4] and J. A. Luna-López[2]

[1] *Instituto de Física, Benemérita Universidad Autónoma de Puebla, Apartado Postal J-48, 72570 Puebla, PUE, Mexico*
[2] *CIDS-ICUAP, Benemérita Universidad Autónoma de Puebla, 14 Sur y Avenida San Claudio, Edificio 137, 72570 Puebla, PUE, Mexico*
[3] *Escuela Superior de Ingeniería Mecánica y Eléctrica Unidad Ticomán, Instituto Politécnico Nacional, 07340 México, DF, Mexico*
[4] *Área Académica de Computación, ICBI, Universidad Autónoma del Estado de Hidalgo, Mineral de la Reforma, Hidalgo, Apartado Postal 42000, Mexico*

Correspondence should be addressed to F. Severiano; pacosc@ifuap.buap.mx

Received 23 September 2013; Revised 11 November 2013; Accepted 6 December 2013; Published 6 January 2014

Academic Editor: Gon Namkoong

Electroluminescent devices (ELD) based on junctions of indium doped zinc oxide (ZnO:In) and porous silicon layers (PSL) are presented in this work. PSL with different thicknesses and photoluminescent emission, around 680 nm, were obtained by anodic etching. PSL were coated with a ZnO:In film which was obtained by ultrasonic spray pyrolysis technique. Once obtained, this structure was optically and electrically characterized. When the devices were electrically polarized they showed stable electroluminescence (EL) which was presented as dots scattered over the surface. These dots can be seen with the naked eye. The observed EL goes from the 410 to 1100 nm, which is formed by different emission bands. The EL emission in the visible region was around 400 to 750 nm, and the emission corresponding to the infrared part covers the 750 to 1150 nm. The electrical characterization was carried out by current-voltage curves *(I-V)* which show a rectifying behavior of the devices. Observed electroluminescent dots are associated with the electron-hole injection into quantized states in PS as well as the emission from the ZnO:In film.

1. Introduction

Crystalline silicon (c-Si) has been a vital material for the development of the microelectronics industry; however, it is an indirect band semiconductor so that it limits its application to the optoelectronics industry. Nevertheless, the discovery of visible luminescence at room temperature of the porous silicon (PS) has reopened the possibility to obtain electroluminescent silicon based devices [1–3]. The discovery of photoluminescence [1] in PS and the understanding of the growth of nanostructures [2] opened the field to a large amount of work on this material. For practical applications, the electroluminescence (EL) is the crucial point. The development of electroluminescent devices (ELD) in PS technology faces some specific problems. The material has a large internal surface; therefore, it shows a tendency to undergo a chemical change when it is exposed to air. Furthermore, nanoporous silicon shows a very low electrical conductivity which causes problems for the EL efficiency. However, ELD with wet contacts [4, 5] have proved to be efficient. This shows that, in principle, PS is a good material to get EL. Most of the ELD present a simple integrated structure of a porous layer and a contact layer on top. For contact, thin metals such as gold, indium tin oxide (ITO), silicon carbide, and conductive polymers are used. An advanced structure has p-n junction within the porous region. For this work, we propose to use a ZnO:In film. ELD with this kind of structure (ZnO:In/SP) has been obtained before but this is the first time that the different components are obtained with techniques of low cost equipment (ultrasonic spray pyrolysis (USP) and anodic etching). Zinc oxide (ZnO) is classified as a semiconductor n-type because it generally has an excess of zinc [6]. ZnO has

an attractive direct gap (3.37 eV) which can be modified to be applied to electrical and optical devices [7]. ZnO:In exhibits both a high optical transmittance in the visible region of the spectrum (between 60 and 80%) and a low resistivity (on the order of 2E-10 Ω-cm) [8] making it an important material in the manufacture of heat mirrors used on gas stoves and also as conductive coating that prevents ice formation on aircraft windows and electrodes in solar cells based on amorphous silicon [9, 10]. The zinc oxide, used in this work, was obtained by ultrasonic spray pyrolysis technique. This method is highly reproducible and can be used at room temperature and for coating large substrates although it does not require a vacuum system. The doped films are stable even when the temperature changes (25–400°C) in the presence of air [11]. Furthermore, ZnO:In thin films do not require extra postannealing treatments in order to obtain low resistivity values in the range of 5×10^{-3} Ω-cm [12]. Due to the characteristics exhibited in these films, we used them as a coating of the PSL.

In this paper, we report fundamental characteristics of a ZnO:In/PS/p-Si diode in terms of the relation between the EL intensity and the operating variables (operation, current density, and thickness of the porous layer) as well as the relation between the EL and PL spectra. This investigation about the EL properties of this kind of structure will help to clarify the EL mechanism of PS-based devices.

2. Experimental Details

PSL were obtained by anodic etching. This process was carried out in a teflon cell designed so that the electrolyte which consists of hydrofluoric acid (HF) and ethanol (CH_3–CH_2–OH) has contact with the c-Si top surface to be attacked. The cathode is formed by a platinum mesh similar in size to the area of the c-Si exposed to the electrolyte. Moreover, the anode is formed by an aluminum (Al) plate. PSL were obtained of c-Si p-type with a resistivity of 2–4 Ω-cm. The used electrolyte was composed of a mixture of hydrofluoric acid (HF) (Merck 40% by volume) and ethanol (CH_3–CH_2–OH) (Alfa-Aesar 99.98% by volume) in a ratio 1 : 2, respectively. The current density to obtain the PSL was 6.49 mA/cm^2; the time of etching was 10, 20, and 30 min.

A laser with a wavelength of 405 nm and 40 mW of power was used to excite the sample in PL measurements of the PSL; the range detected by the monochromator was from 400 to 1100 nm. The thickness of the PSL was estimated by gravimetry; the thickness obtained by this method was compared with physical measurements performed by profilometry.

The thickness of the PSL was obtained by the expression [13, 14]

$$E = \frac{m_1 - m_2}{\rho A_a}, \quad (1)$$

where m_1 is the mass of the wafer of c-Si before the attack, m_2 is the mass of the same wafer after removing the porous layer, ρ is the density of the c-Si (in g/cm^3), and A_a is the attacked area during the anodization (in cm^2).

The thickness of the PSL was measured by a Dektak 150 profilometer (this equipment allows measuring film thicknesses below 100 Å). This analysis was conducted after the porous layer was removed using a solution of NaOH.

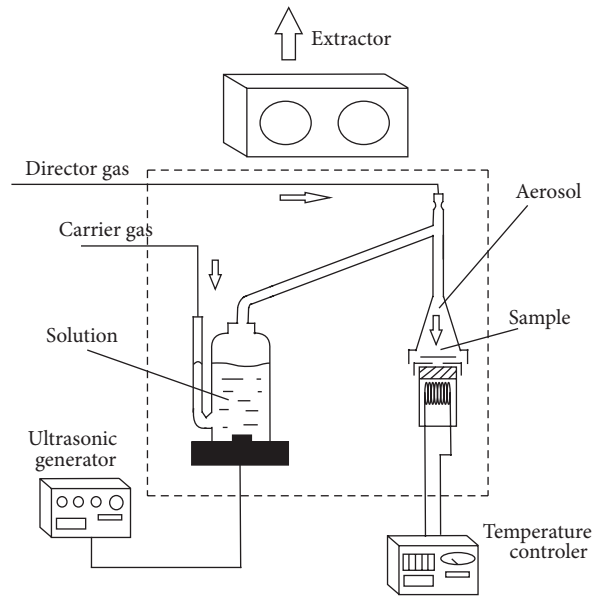

Figure 1: Schematic diagram of the experimental setup used for depositing the ZnO:In thin films.

ZnO:In thin solid films were prepared using the ultrasonic spray pyrolysis (USP) technique which is a versatile technique that can be used to produce nanoscale sized powders and thin solid films. The deposition system used to obtain the ZnO:In thin film presented in this work includes a piezoelectric transducer which operates at variable frequency and that was set to 1.2 MHz and the ultrasonic power at 120 W. ZnO:In thin films were deposited from a 0.2 M solution of zinc acetate ($[Zn(O_2CCH_3)_2]$ from Alfa, 98%), dissolved in a mix of deionized water, acetic acid ($[CH_3CO_2H]$ from Baker, 95%), and methanol ($[CH_3OH]$ from Baker, 98%). Separately, a 0.2 M solution of indium acetate ($[In(CH_3CO_2)_3]$ from Alfa, 98%) dissolved in a mix of deionized water and acetic acid (1 : 1, volume proportion) was prepared in order to be used as a doping solution. The substrate temperature (Ts) was kept constant at 430°C. Pure N_2 (from PRAXAIR, 99.997%) was used as solution carrier and a director gas with flow rates of 3.5 and 0.5 L·min^{-1}, respectively. Figure 1 shows a schematic diagram of the experimental setup used for depositing the ZnO:In thin films (ultrasonic spray pyrolysis: USP).

The thickness of the ZnO:In thin films was measured by a KLA profilometer (Tencor model P15 with a resolution of 1.5 nm) from a step formed during deposition. All the samples were grown with a film thickness value of 600 nm approximately. The microcrystalline structure of the samples was studied with X-ray diffraction analysis, obtained in a Siemens D5000 diffractometer by using the Cu-K1 (λ = 0.154056 nm) radiation and the θ-2θ technique. The optical transmittance spectra at normal incidence of the ZnO:In film were obtained by a double-beam Shimadzu 2401 PC spectrophotometer in the UV-Vis region (350–1000 nm) without glass substrate correction. Electrical sheet resistance of the ZnO:In was

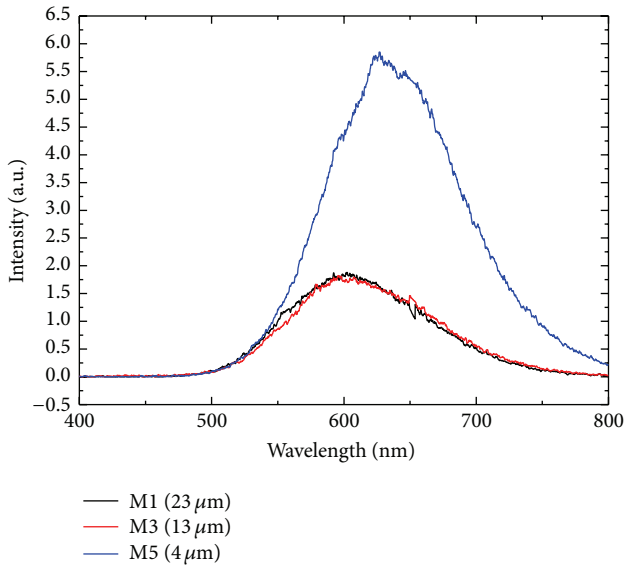

Figure 2: PL spectra for the PSL utilized to get the ELD.

measured by the conventional four-aligned probe method (Veeco equipment) with the appropriate geometric correction factors.

The optical characterization of the ELD was obtained with a monochromator model iHR320 HORIBA brand Jobin Yvon which is coupled to a CCD detector model iHR320 brand Synapse; the range detected by the monochromator was from 300 to 1100 nm. The resolution of this equipment is 0.06 nm, whereas the scanning speed is 160 nm/seg and an accuracy of 0.20 nm wavelength. EL spectra were obtained by applying different currents of operation to the device. The electrical characterization was carried out with a Keithley 2000 multimeter through which variable current was applied to ELD; the data were monitored by a LabTracer program through which current-voltage (I-V) curves were obtained.

3. Results and Discussions

3.1. PL of PS. We proceeded to get three samples with different thicknesses to obtain the ELD and carry out the proposed study. Figure 2 shows the result of the optical analysis performed. The used electrochemical etching current was of 6.49 mA/cm^2; this current was selected because it had shown the highest PL intensity in previous analyses. The obtained sample with this current density showed the highest PL intensities because this current favors the obtaining of silicon filaments that are emitted in the visible region. The etching times were 10, 20, and 30 min, corresponding to thickness of 4(M5), 13(M3), and 23(M1) μm, respectively. Figure 2 shows that, by increasing the anodized time, the maxima of the curves show a shift to higher energies and it is observed that the peaks intensity decreases. This shift goes from 650 to 600 nm. This is due to the reduction of the emitting silicon filaments size present in the PS structure [15], and the intensity decrease is the result of the oxidation process which takes place in the PSL [16]. This process reduces the filament size until the filaments lose their capacity to emit light. As it can be seen the samples show an increase in the PL inversely proportional to the thickness of the PSL. This is the typical behavior of this kind of samples. These three samples were used in obtaining the devices.

Table 1: Thickness of the PSL obtained by gravimetry and profilometry.

Sample	Thickness (μm)	Profilometry (μm)
M1	23	21
M3	13	12
M5	4	3.5

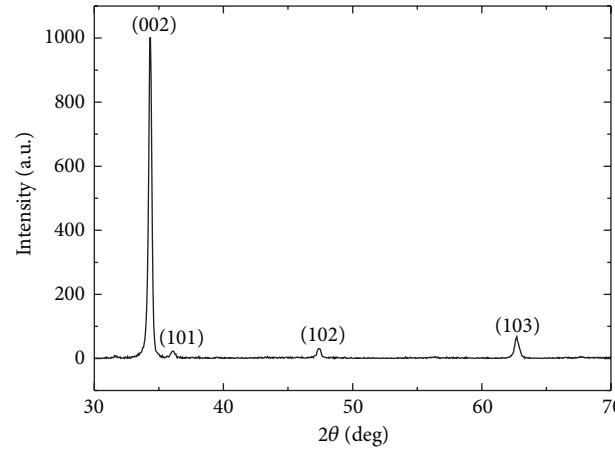

Figure 3: Diffraction pattern of the ZnO:In film deposited at 430°C.

3.2. Thickness of the PSL. Table 1 shows the thicknesses of the PSL (obtained with a current density of 6.49 mA/cm^2) calculated by (1) and the profilometry results. We can see that the results between gravimetry and profilometry show good agreement (±5%).

3.3. ZnO:In Characterization. ZnO:In film was obtained from the precursor solution as it was described before, the Ts was kept constant at 430°C, and time growth was 10 minutes in all cases. This is the temperature of the PSL when the ZnO:In film was deposited to get the devices. X-ray diffraction patterns obtained from ZnO:In thin films show polycrystalline characteristics and the corresponding peaks fit well to a hexagonal ZnO:In wurtzite type structure. Figure 3 shows the pattern of ZnO:In thin films.

The crystallite size was estimated using the (002) and (100) diffraction peaks from the XRD data in accordance with the Debye-Scherer formula [17]. According to the results, the crystallite size of the ZnO:In thin films is around 23 to 36 nm.

Figure 4 shows the optical transmittance spectra of ZnO:In thin film deposited on soda-lime glass substrate. No substrate correction was made to the corresponding measurement. Average transmittance of the obtained film is suited for transparent conductive oxide (TCO) application. Optical band gap was calculated from the plot of $(\alpha h\nu)^2$ as a function

Table 2: ZnO:In films electric resistivity.

Sample	Average thickness (nm) ±5.0%	Average transmittance (400–700 nm) (%)	Electrical resistivity $\times 10^{-3}$ (Ωcm) ±5.0%	Band gap (eV) ±5.0%
ZnOIn/SLGS	685	53.11	2.05	3.44

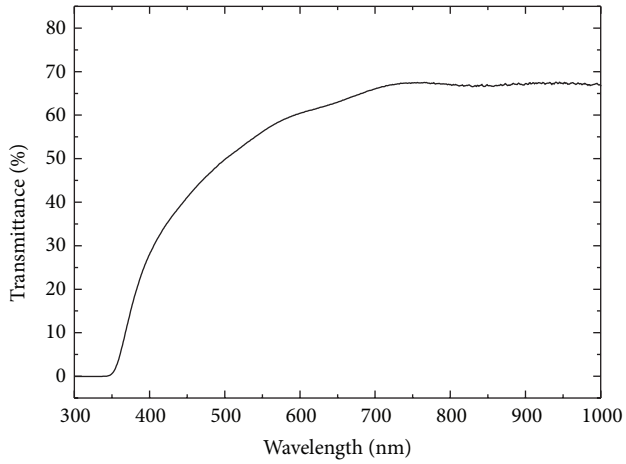

Figure 4: The optical transmittance is about 53%.

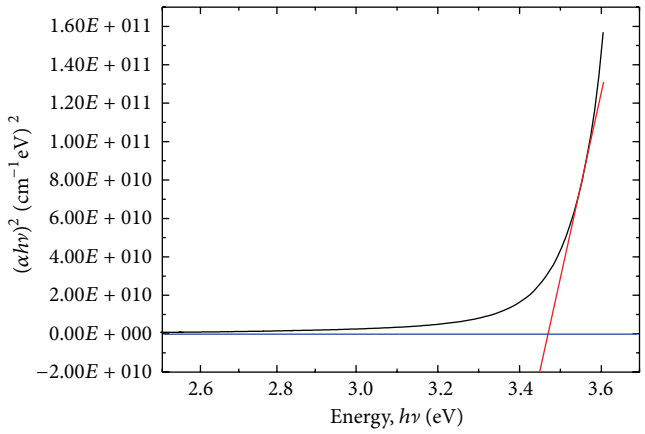

Figure 5: Plot of $(\alpha h\nu)^2$ versus $h\nu$ and estimate of the band gap.

of $h\nu$, where α is the optical absorption coefficient and $h\nu$ is the energy of the incident photons. From these curves, the optical band gap (Eg) values can be estimated by the extrapolation of straight line to $(\alpha h\nu) = 0$. Figure 5 shows band gap value (3.44 eV).

Table 2 shows the electrical resistivity value and the principal characteristics for ZnO:In thin film deposited on soda-lime glass substrate (SLGS). Electrical sheet resistance of the sample was measured by the conventional four-aligned probe method.

Both optical and electrical characterization show that the ZnO:In films possess the necessary properties to be used as an electrical contact and as a transparent coating to get ELD based on PSL.

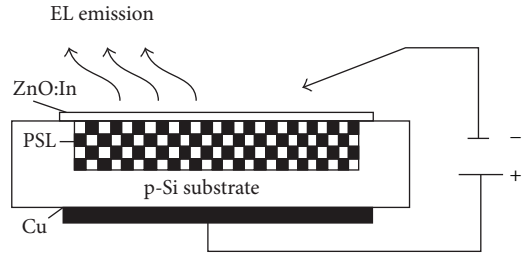

Figure 6: Schematic diagram of the ELD structure.

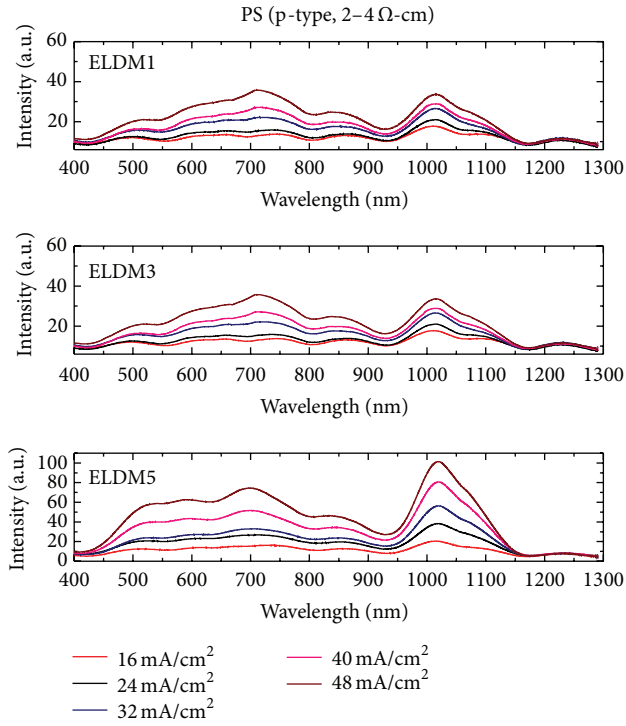

Figure 7: EL spectra obtained from the ELD. We can see the response of the device with different current densities.

4. Results and Discussion of ELD

Figure 6 shows the distribution of the components of the ELD. EL responses were obtained from devices taken by applying DC current. The negative terminal was connected to the ZnO:In film through a needle probe (we say that our device is forward polarized); the device presented luminescent spots on the surface which were visible to the naked eye.

Figure 7 shows the EL spectra of the ELD labeled ELDM1, ELDM3, and ELDM5 which have thicknesses of 23, 13 and 4 μm, respectively. In the spectra we can see that the EL

emission goes from 400 to 1100 nm for all samples and the EL intensity increases with the increasing of the operating current density. Based on the spectra and the images taken from the devices, the emitted light is white. The sample that showed the best performance in the visible and infrared part was the sample labeled as ELDM5 (4 μm). In the visible part of the spectra three principal peaks centered at 500, 600, and 710 nm are seen, and in the infrared region one principal peak centered at 1020 nm is observed. The emissions observed in the visible region are attributed to the PS and the ZnO:In film. The emission centered at 600 nm is due to the presence of silicon filaments which have different diameters (nanosized) and that are present in the PS as we can see in the PL characterization. This changes their bandwidth and thereby the wavelength that is emitted [18–21]. The emission centered at 500 is the characteristic blue-green (BG) emission band (broad fluorescence band) typically observed in ZnO films, and it is due to the transition from the conduction band to the O_{zn} level [22]. The peak at 710 nm might be due to the emission from a level caused by oxygen interstitials attributed to ZnO:In; the measure of the peaks associated with the ZnO film was performed by Castañeda in previous works [22]. The emission that is observed in the IR might be due to the crystalline silicon substrate, since there are reports which say that the silicon is emitted in that region [18, 23]. This would explain the fact that the corresponding emission to this region is increased to reduce the thickness of the porous film, allowing the contribution of the substrate to be observed in a better way when the device is polarized. Comparing the obtained results of PL and EL, we can conclude that the intensity of the EL emission of the devices is directly related to the PL than the PSL present. This is evident since the EL intensity is directly related to the PL behavior; as it can be seen in Figure 2, the sample with the highest PL intensity is the same sample with higher EL intensity. The sample that showed the best PL and EL was the sample with a thickness of 4 μm; this is due to the high concentration of emitting filaments present in this sample which is reflected in the intensity of the spectra obtained. Through the analysis of the obtained results, we can observe that in order to improve the functioning of this kind of devices, we have to find the way to improve the PL of PS.

4.1. Comparison between PL and EL. Figure 8 shows a comparison between the PL and EL spectra obtained from ELDM5 device. This gives us evidence to explain the origin of emissions in the devices. In the PL spectra of the ELD, emissions that are from 400 to 800 nm are related to the PS and the ZnO:In film. Figure 2 shows that the main peak of PS emission is around the 600 nm, and as we said before there are works that report emissions from ZnO:In in 500 and 710 nm. This explains the observed peaks in the PL spectra of the ELD (black in Figure 8). Now if we compare the PL and the EL spectra of the ELD, the EL spectra show a main peak around 1020 nm. We related this emission to the silicon substrate. The IR band cannot be observed in the PL because the laser penetrates only slightly in the sample [24]; moreover, the electric current goes through the entire sample, exciting also the substrate; for this reason the silicon substrate can only be appreciated in the EL spectra.

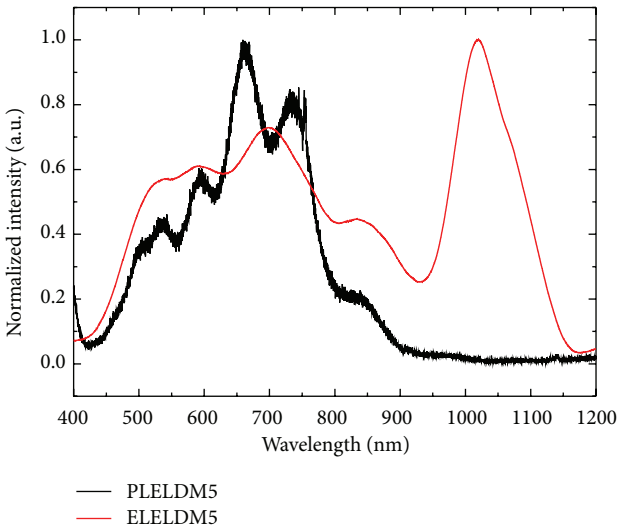

Figure 8: Comparison between PL and EL spectra of the ELD.

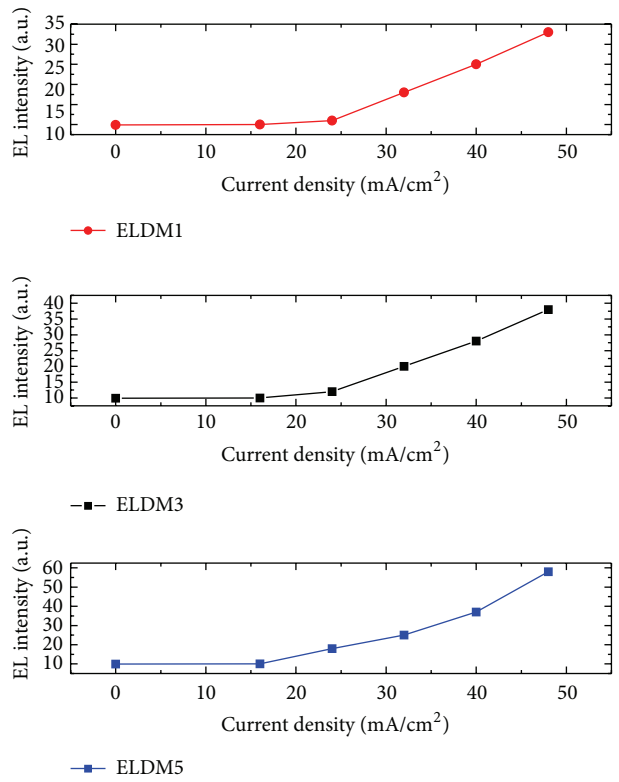

Figure 9: Plot of EL versus operation current density. We can see two regions which exhibit a linear relationship.

4.2. EL Analysis

4.2.1. Relation between EL Intensity and Current Density. Figure 9 shows the behavior of the EL as a function of the

operating current density applied to the obtained devices. The graph shows that the EL intensity increases when increasing the operation current density; this behavior is observed in all the studied samples.

We can see two regions which exhibit a linear relationship; the first region goes from 0 to 15 mA/cm^2 and the second region goes from 15 to 48 mA cm^2. This denies the direct excitation of luminescence centers by accelerated carriers as the EL principal excitation mechanism. This suggests that the localized electron-hole pairs are responsible for the visible EL which is created by trapping an electron and hole from the conduction and the valence band, respectively [25]. The deviation from the linear relationship at low current densities implies that there is some current component which does not directly contribute. In other words, a significant amount of current precedes the onset of EL.

4.3. EL Source. On the basis of the PL and EL spectra, and the relation between EL intensity and current density analysis, we can conclude that the observed white EL is a combination of red emission from the PS and blue light from the ZnO:In layer when it is excited by the operating current density. In the PS, each emitting filament is supposed to be surrounded by a wide band gap region since it behaves like a quantum dot [26]. The wide gap region may be composed of oxides, hydrides, amorphous Si, or simply a Si nanostructure of smaller dimensions. Thus, the microscopic structure of PS along the direction of current flow can be understood as if the Si nanocrystallites are connected together via wider gap interface regions. When a bias voltage is applied to this ensemble, a stronger electric field may build up preferentially in the wide-gap regions because of their expected lower dielectric constant and higher resistivity. Then, the conduction and valence band edges of the nanocrystallites become shifted with respect to those of respective neighboring ones. This band shift increases when the applied voltage rises. Therefore, under a sufficient high voltage bias, a critical situation would appear locally: the energy position of the valence-band edge of a crystallite becomes comparable with that of the conduction band edge of the neighboring one. In this situation, either of the following two phenomena is expected to occur. First, hot electrons injected from the conduction band of the neighboring one are so energetic that they can create electron-hole pairs by an impact process (process 1). Second, electron-hole pairs can be created also by the tunneling of electrons from the valence band of a crystallite into the conduction band of the next one (process 2). Progress of these processes should significantly increase the number of carriers in the PSL and consequently let a sharp increase in current density at the corresponding voltage. This is similar to the electrical breakdown in reverse biased p-n junctions. Otherwise the electric current excites the oxygen interstitials in the ZnO:In film which originates the blue light that can be seen in the PL and EL spectra.

4.4. Electrical Characteristics of the DEL. Figure 10 shows the obtained *I-V* curves from the devices. This is a typical *I-V* curve for a ZnO:In/PS/p-Si structure which shows characteristic rectification behavior. The forward direction corresponds to a negative potential on the ZnO:In film. From a forward voltage of around 15 V, spots of white light could be seen by the naked eye in a dimly lit room which merged together as the bias was increased. Closer examination of the EL at lower potentials (approximately 10–15 V) revealed that in addition to the white light small spots on the surface, they emitted red light. At higher current densities, only white light was observed; however, it was not possible to ascertain whether this was due to the previously red spots now emitting white light or if the more intense white light from other regions was simply masking the colored EL from these areas. No light emission was observed under reverse bias.

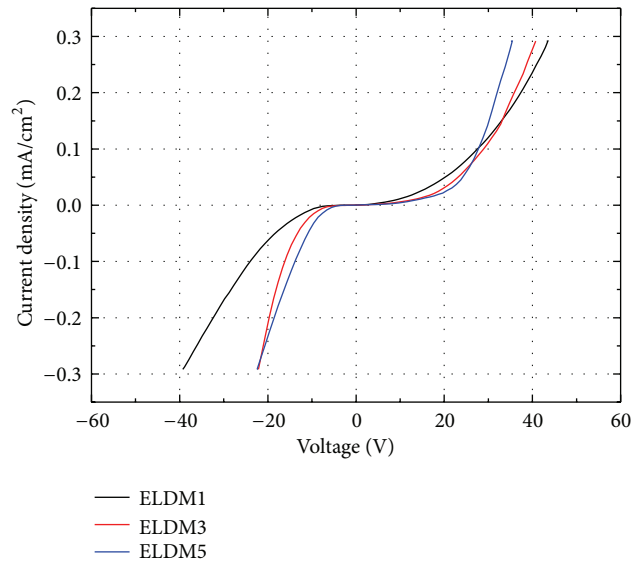

Figure 10: *I-V* curves for devices obtained. This is a typical *I-V* curve that shows rectification behavior.

5. Conclusions

ELD from structures based on ZnO:In/SP which exhibit emission in the visible and infrared region of the electromagnetic spectrum were obtained. We demonstrated stable white light emission from ZnO:In/PS structures through EL and PL spectra. The device presented luminescent spots on the surface which were visible to the naked eye. It was shown that the EL emission is related to the PL behavior of the PSL used to obtain the devices. It was proved that the EL emission is integrated by the emission of ZnO:In, PS, and the silicon substrate. Also the results indicate that the thickness of the porous layer is very important in the electrical behavior because the devices tend to behave as a diode.

Conflict of Interests

The authors declare that there is no conflict of interests regarding the publication of this paper.

Acknowledgments

F. Severiano thanks CONACyT for its support through 33741 studentship. Heberto Gómez-Pozos acknowledges financial support from the Programa de Mejoramiento del Profesorado from the SEP México through Project no. PROMEP/103.5/11/0144. The authors also acknowledge S & C Associates for proof-reading of the paper.

References

[1] L. T. Canham, "Silicon quantum wire array fabrication by electrochemical and chemical dissolution of wafers," *Applied Physics Letters*, vol. 57, no. 10, pp. 1046–1048, 1990.

[2] V. Lehmann and U. Gösele, "Porous silicon formation: a quantum wire effect," *Applied Physics Letters*, vol. 58, no. 8, pp. 856–858, 1991.

[3] C. Pickering, M. I. J. Beale, D. J. Robbins, P. J. Pearson, and R. Greef, "Optical studies of the structure of porous silicon films formed in p-type degenerate and non-degenerate silicon," *Journal of Physics C*, vol. 17, no. 35, pp. 6535–6552, 1984.

[4] J. C. Vial, A. Bsiesy, F. Gaspard et al., "Mechanisms of visible-light emission from electro-oxidized porous silicon," *Physical Review B*, vol. 45, no. 24, pp. 14171–14176, 1992.

[5] A. Bsiesy, F. Muller, M. Ligeon et al., "Optical properties of low dimensional silicon structures," in *Proceedings of the NATO Advanced Research Workshop*, Meylan, France, 1993.

[6] T. Okamura, Y. Seki, S. Nagakari, and H. Okushi, "Junction properties and gap states of ZnO thin film prepared by sol-gel process," *Japanese Journal of Applied Physics*, vol. 31, pp. 3218–3220, 1992.

[7] L. Castañeda, A. García-Valenzuela, E. P. Zironi, J. Cañetas-Ortega, M. Terrones, and A. Maldonado, "Formation of indium-doped zinc oxide thin films using chemical spray techniques: the importance of acetic acid content in the aerosol solution and the substrate temperature for enhancing electrical transport," *Thin Solid Films*, vol. 503, no. 1-2, pp. 212–218, 2006.

[8] A. Guillen-Santiago, M. D. L. L. Olvera, and A. Maldonado, "Películas delgadas de ZnO:F depositadas por rocío químico: efecto de la temperatura de substrato sobre las propiedades físicas," *Superficies y Vacio*, vol. 13, pp. 77–79, 2001.

[9] K. L. Chopra, S. Major, and D. K. Pandya, "Transparent conductors—a status review," *Thin Solid Films*, vol. 102, no. 1, pp. 1–46, 1983.

[10] M. A. Martínez, J. Herrero, and M. T. Gutiérrez, "Deposition of transparent and conductive Al-doped ZnO thin films for photovoltaic solar cells," *Solar Energy Materials and Solar Cells*, vol. 45, no. 1, pp. 75–86, 1997.

[11] P. S. Patil, "Versatility of chemical spray pyrolysis technique," *Materials Chemistry and Physics*, vol. 59, no. 3, pp. 185–198, 1999.

[12] J. F. Guillemoles, D. Lincot, P. Cowache, and J. Vedel, "Solvent effect on ZnO thin films prepared by spray pyrolysis," in *Proceedings of the 10th European Photovoltaic Solar Energy Conference*, A. Luque, G. Sal, W. Pals, G. dos Santos, and P. Helm, Eds., pp. 609–612, Lisbon, Portugal, 1991.

[13] J. J. Yon, K. Barla, R. Herino, and G. Bomchil, "The kinetics and mechanism of oxide layer formation from porous silicon formed on p-Si substrates," *Journal of Applied Physics*, vol. 62, no. 3, pp. 1042–1048, 1987.

[14] Z. Fekin, F. Z. Otmani, N. Ghellai, and N. E. Chabanne-Sari, "Characterization of the porous silicon layers," *The Moroccan Journal of Condensed Matter*, vol. 7, no. 1, pp. 35–37, 2006.

[15] P. Kumar, "Effect of silicon crystal size on photoluminescence appearance in porous silicon," *ISRN Nanotechnology*, vol. 2011, Article ID 163168, 6 pages, 2011.

[16] R. Herino, "Luminescence of porous silicon after electrochemical oxidation," in *Porous Silicon Science and Technology*, pp. 53–66, 1995.

[17] B. E. Warren, *X-Ray Diffraction*, Dover, New York, NY, USA, 1990.

[18] T. P. Pearsall, J. C. Adams, J. N. Kidder Jr. et al., "Bright visible photoluminescence in thin silicon films," *Thin Solid Films*, vol. 222, no. 1-2, pp. 200–204, 1992.

[19] W. Lang, P. Steiner, and F. Kozlowski, "Porous silicon electroluminescent devices," *Journal of Luminescence*, vol. 57, pp. 341–349, 1993.

[20] G. Hu, S. Q. Li, H. Gong et al., "White light from an indium zinc oxide/porous silicon light-emitting diode," *The Journal of Physical Chemistry C*, vol. 113, no. 2, pp. 751–754, 2009.

[21] Y. Zhao, D. Yang, L. Lin, and D. Que, "Blue light emission of porous silicon subjected to RTP treatments," *Chinese Science Bulletin*, vol. 51, no. 22, pp. 2696–2699, 2006.

[22] L. Castañeda, O. G. Morales-Saavedra, J. C. Cheang-Wong et al., "Influence of indium concentration and substrate temperature on the physical characteristics of chemically sprayed ZnO:In thin films deposited from zinc pentanedionate and indium sulfate," *Journal of Physics Condensed Matter*, vol. 18, no. 22, pp. 5105–5120, 2006.

[23] S. S. Iyer and Y.-H. Xie, "Light emission from silicon," *Science*, vol. 40, pp. 40–46, 1993.

[24] N. Koshida, H. Koyama, Y. Suda et al., "Optical characterization of porous silicon by synchrotron radiation reflectance spectra analyses," *Applied Physics Letters*, vol. 63, pp. 2774–2776, 1993.

[25] T. Oguro, H. Koyama, T. Ozaki, and N. Koshida, "Mechanism of the visible electroluminescence from metal/porous silicon/n-Si devices," *Journal of Applied Physics*, vol. 81, no. 3, pp. 1407–1412, 1997.

[26] S. Schuppler, S. L. Friedman, M. A. Marcus et al., "Dimensions of luminescent oxidized and porous silicon structures," *Physical Review Letters*, vol. 72, no. 16, pp. 2648–2651, 1994.